

## Neutron scattering study of hydrogen dynamics in $\text{Pr}_2\text{Fe}_{17}\text{H}_5$

E. Mamontov,<sup>1,2</sup> T. J. Udovic,<sup>1</sup> O. Isnard,<sup>3,4</sup> and J. J. Rush<sup>1</sup><sup>1</sup>*NIST Center for Neutron Research, National Institute of Standards & Technology, 100 Bureau Drive, MS 8562, Gaithersburg, Maryland 20899-8562, USA*<sup>2</sup>*Department of Materials Science and Engineering, University of Maryland, College Park, Maryland 20742-2115, USA*<sup>3</sup>*Laboratoire de Cristallographie, CNRS, associé à l'Université J. Fourier, Boîte Postale 166X, F-38042 Grenoble Cedex, France*<sup>4</sup>*Institut Universitaire de France, Maison des Universités, 103 Boulevard Saint-Michel, F-75005 Paris Cedex, France*

(Received 26 July 2004; published 22 December 2004)

$\text{Pr}_2\text{Fe}_{17}\text{H}_5$  is an interesting compound where isolated hexagons formed by the tetrahedral sites of the host metal lattice are filled with hydrogen atoms. A localized jump diffusion of hydrogen atoms in  $\text{Pr}_2\text{Fe}_{17}\text{H}_5$  over the vertices of the hexagons is observed using quasielastic neutron scattering. The hydrogen hopping occurs despite the repulsive interaction due to the presence of two hydrogen atoms per hexagon. The residence time of hydrogen atoms between jumps follows an Arrhenius-type law with an activation energy of 0.14 eV. The hydrogen atoms in the octahedral sites are found to be immobile on the time scale of the measurement.

DOI: 10.1103/PhysRevB.70.214305

PACS number(s): 66.30.-h

### I. INTRODUCTION

Most of the  $R_2\text{Fe}_{17}$  compounds are ferromagnetic with moderate Curie temperatures. Insertion of light elements, in particular, hydrogen, leads to dramatic changes in the magnetic properties of these materials. Hydrogenated  $R_2\text{Fe}_{17}$  compounds show a spectacular increase in Curie temperature and magnetization, which have made them attractive candidates for hard magnet materials.<sup>1-3</sup> In this work, we use neutron scattering to investigate the dynamics of hydrogen in  $\text{Pr}_2\text{Fe}_{17}\text{H}_5$ . The interesting magnetic properties of this compound have been the subject of several studies.<sup>4-7</sup> Similar to other  $R_2\text{Fe}_{17}$  compounds with the lighter rare-earth atoms,  $\text{Pr}_2\text{Fe}_{17}$  crystallizes in the  $\text{Th}_2\text{Zn}_{17}$  rhombohedral  $R\text{-}3m$  structure.<sup>8</sup> While the host metal structure is retained, hydrogen insertion is accompanied by an anisotropic increase of the lattice parameters. In the course of hydrogenation, the first three hydrogen atoms fully occupy the interstitial  $9e$  distorted octahedral sites, with four Fe atoms and two Pr atoms at the corners.<sup>9</sup> In  $\text{Pr}_2\text{Fe}_{17}\text{H}_x$  with  $x > 3$ , in addition to the octahedral sites, hydrogen atoms partially occupy interstitial  $18g$  tetrahedral sites, with two Fe atoms and two Pr atoms at the corners.<sup>8</sup> Based on the structural refinement data at 300 K,<sup>8</sup> the tetrahedral sites in the basal plane can be viewed as arrays of isolated hexagons, with a side dimension of  $\approx 1.16 \text{ \AA}$ , and a separation between the hexagons' centers of  $\approx 8.70 \text{ \AA}$  equal to the lattice constant  $a$  (see Fig. 1). The small size of the hexagons may explain why the maximum hydrogen uptake corresponds to  $x=5$ . In this case, one-third of the available  $18g$  tetrahedral sites in  $\text{Pr}_2\text{Fe}_{17}\text{H}_5$  are occupied. According to Switendick's empirical criterion,<sup>10</sup> the minimum attainable H-H separation in ordered metal hydrides is  $\approx 2.1 \text{ \AA}$ , an effect which is ascribed to a repulsive interaction. A recently found exception is a series of  $R\text{NiIn}$  hydrides ( $R=\text{La}, \text{Ce}, \text{Nd}$ ), where short separations between pairs of H atoms ( $1.562\text{--}1.635 \text{ \AA}$ ) have been attributed to the reduction of the repulsive interaction due to polarization of the electron distribution at the H sites toward  $R$  and In atoms.<sup>11,12</sup> It is proposed by Isnard *et al.*<sup>3</sup> that two hydrogen

atoms occupy two diametrically opposite vertices of the hexagons in  $\text{Pr}_2\text{Fe}_{17}\text{H}_5$ . This is because all but the opposite vertices of these hexagons, which possess a side dimension of  $1.16 \text{ \AA}$ , are too close to accommodate a pair of hydrogen atoms. Since hydrogen is very mobile, it can be expected that the hydrogen atoms jump between the available sites comprising each hexagon. Fast localized motion of H atoms within hexagons has been observed in several nonstoichiometric Laves phase compounds.<sup>13-16</sup> However,  $\text{Pr}_2\text{Fe}_{17}\text{H}_5$  is qualitatively different from these nonstoichiometric hydrides because of the high population of two H atoms per hexagon. In this case, the repulsive interaction may be expected to block the hydrogen hopping. We used vibrational neutron spectroscopy and quasielastic neutron scattering to assess the dynamics of hydrogen in  $\text{Pr}_2\text{Fe}_{17}\text{H}_5$ . Thanks to a very large neutron incoherent scattering cross section of hydrogen, neutron scattering is ideally suited to probe the dynamics of hydrogen motion. The results of our quasielastic neutron scattering (QENS) experiments demonstrate that hydrogen atoms in  $\text{Pr}_2\text{Fe}_{17}\text{H}_5$  perform jumps between the available tetrahedral sites in spite of the presence of two hydrogen atoms per hexagon. The temperature dependence of the time be-

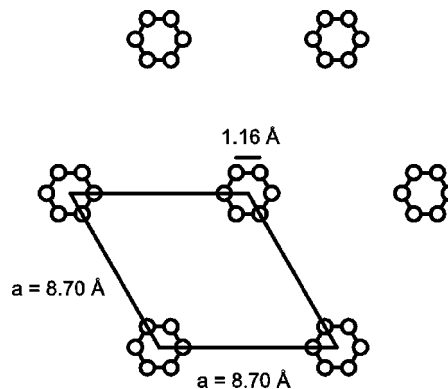


FIG. 1. Arrays of hexagons formed by the tetrahedral sites in the basal plane of  $\text{Pr}_2\text{Fe}_{17}\text{H}_5$ . Two hydrogen atoms occupy a hexagon in  $\text{Pr}_2\text{Fe}_{17}\text{H}_5$ , whereas in  $\text{Pr}_2\text{Fe}_{17}\text{H}_3$  the hexagons are empty.

tween jumps exhibits an Arrhenius-type behavior with an activation energy of 0.14 eV. The hydrogen atoms in the octahedral sites appear immobile on the timescale of the QENS measurements.

## II. EXPERIMENT

The synthesis procedure for  $\text{Pr}_2\text{Fe}_{17}$  samples has been described elsewhere.<sup>7,17,18</sup> Hydrogen was loaded by means of gas absorption. Neutron scattering experiments were carried out at the NIST Center for Neutron Research. Vibrational spectroscopy measurements were performed with the filter-analyzer neutron spectrometer<sup>19</sup> using the Cu(220) monochromator and horizontal collimations of 20 and 40 min of arc before and after the monochromator, respectively. QENS measurements were performed with the high-flux back-scattering spectrometer<sup>20</sup> (HFBS) and the time-of-flight disc chopper spectrometer<sup>21</sup> (DCS). The HFBS provides  $\approx 1 \mu\text{eV}$  energy resolution at a fixed final wavelength of 6.27 Å, while a variation of the incident wavelength is achieved by means of using a Si(111) monochromator mounted on a mechanical Doppler drive. With a fixed final wavelength, the values of the scattering momentum transfer  $Q$  are then defined by the detector positions. For the DCS measurement, we used a wavelength of 5 Å. At this incident wavelength, the intermediate-resolution operation mode of the instrument provides an energy resolution of about 63  $\mu\text{eV}$  [full width at half maximum (FWHM)], as measured with the sample at 30 K. To improve the statistics for data analysis, the data covering the range of the scattering vectors  $0.70 \text{ \AA}^{-1} < Q < 2.20 \text{ \AA}^{-1}$  (at the elastic channel) have been summed and rearranged to yield 13 spectra with constant-energy binning of the data points for the energy range of  $\pm 600 \mu\text{eV}$ . For all neutron measurements, the sample was placed in an annular Al sample holder in a He atmosphere, sealed with an indium o-ring, and mounted onto a closed-cycle refrigerator. The thickness of the container was chosen to ensure 90% neutron transmission through the sample and thus minimize multiple scattering. The temperature of the refrigerator was controlled within  $\pm 1$  K. The data were collected at 390 and 30 K with the DCS and at 260, 240, 220, 200, and 20 K with the HFBS. The scattering spectra measured at the lowest temperatures were used as resolution functions. In addition, a special fixed-window operation mode of the HFBS was used while the sample temperature was ramped down from 300 to 5 K at a rate of 1 K/min. In this mode, the Doppler drive is stopped, and the elastic scattering intensity is collected as a function of sample temperature or other time-dependent parameter. The energy resolution of the HFBS in this mode of operation is about 0.8  $\mu\text{eV}$ .

## III. RESULTS AND DISCUSSION

Figure 2 shows the 10 K vibrational spectra for  $\text{Pr}_2\text{Fe}_{17}\text{H}_3$  and  $\text{Pr}_2\text{Fe}_{17}\text{H}_5$ . While a more detailed analysis of the vibrational spectra will be presented elsewhere,<sup>22</sup> it is sufficient to note that the spectra are consistent with the location of hydrogen atoms in the octahedral and tetrahedral sites previously determined by neutron diffraction.<sup>8</sup> The two main

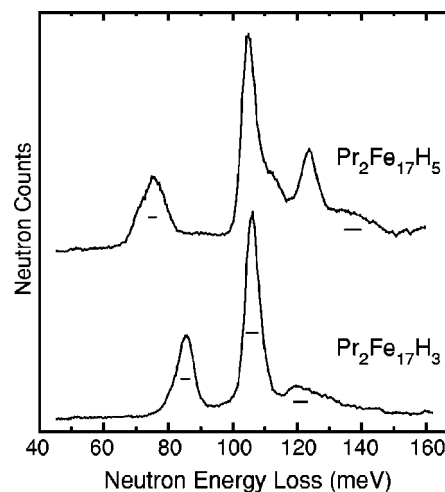


FIG. 2. The neutron vibrational spectra of  $\text{Pr}_2\text{Fe}_{17}\text{H}_3$  and  $\text{Pr}_2\text{Fe}_{17}\text{H}_5$  measured at 10 K. The resolution (FWHM) is denoted by the horizontal bars beneath the spectra.

peaks in the  $\text{Pr}_2\text{Fe}_{17}\text{H}_3$  spectrum centered at  $\approx 85.4$  and 106.0 meV reflect the vibrations of the hydrogen atoms in the octahedral sites. In  $\text{Pr}_2\text{Fe}_{17}\text{H}_5$ , these peaks shift to lower energies of  $\approx 75.3$  and 104.7 meV. The observed mode softening is induced by the presence of the additional H atoms in the tetrahedral sites, and the resulting expansion of the lattice. Two new peaks in the  $\text{Pr}_2\text{Fe}_{17}\text{H}_5$  spectra at  $\approx 112$  meV (which appears as a shoulder of a stronger peak) and 123.7 meV are assigned to the vibrations of the hydrogen atoms in the tetrahedral sites. Other features in the spectra originate from optical or optoacoustic multiphonon scattering.

Figure 3 illustrates the temperature dependence of the elastic scattering intensity for  $\text{Pr}_2\text{Fe}_{17}\text{H}_3$  and  $\text{Pr}_2\text{Fe}_{17}\text{H}_5$  obtained using the fixed-window operation mode of the HFBS as described above. The general trend for both samples is a gradual increase of the scattering intensity as temperature is decreased. This is due to the temperature dependence of the Debye-Waller factor, and possibly, progressive trapping of mobile hydrogen at low temperatures. For  $\text{Pr}_2\text{Fe}_{17}\text{H}_5$ , there exists a distinctive region below  $\sim 170$  K, where the elastic

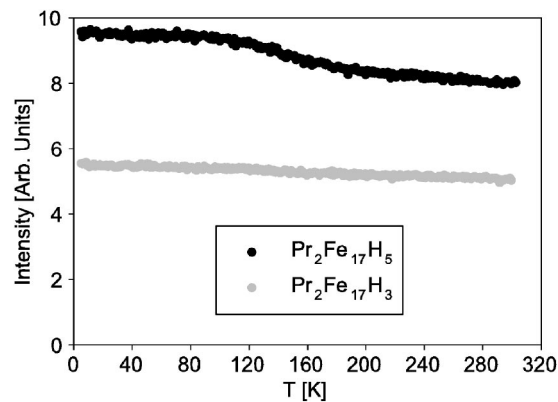


FIG. 3. The temperature dependence of the elastic scattering intensity for  $\text{Pr}_2\text{Fe}_{17}\text{H}_3$  and  $\text{Pr}_2\text{Fe}_{17}\text{H}_5$  obtained using the fixed-window operation mode of the HFBS.

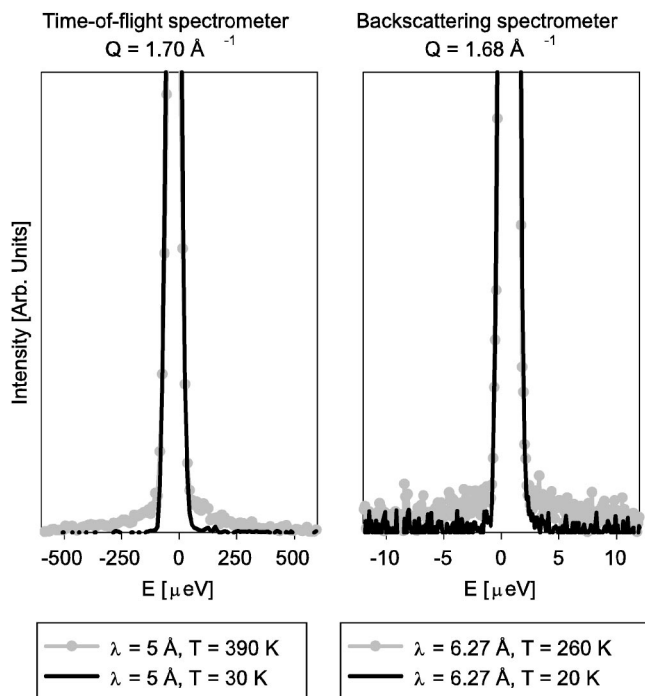


FIG. 4. Examples of QENS spectra obtained with the time-of-flight ( $\lambda=5 \text{ \AA}$ ) and backscattering ( $\lambda=6.27 \text{ \AA}$ ) spectrometers. The low-temperature data represent the resolution functions.

scattering intensity grows more rapidly as the temperature is decreased. This is indicative of the fact that the dynamics of hydrogen motion, which slows down with decreasing temperature, becomes too slow for the  $0.8 \mu\text{eV}$  resolution of the spectrometer. This “freezing” of the hydrogen motion on the time scale of the spectrometer increases the elastic signal. On the other hand, there is no such change in the dynamics of hydrogen in  $\text{Pr}_2\text{Fe}_{17}\text{H}_3$ . Therefore, the quasielastic broadening in the microelectronvolt range at  $T > 170 \text{ K}$  can be ascribed to the hydrogen atoms in the tetrahedral sites, whereas those in the octahedral sites appear immobile on the timescale of the spectrometer ( $\approx 0.8 \text{ ns}$ ). It should be noted that the ratio of the elastic intensities for the two samples measured at  $T=5 \text{ K}$  is close to 5:3, as one expects for  $\text{Pr}_2\text{Fe}_{17}\text{H}_x$  with  $x=3$  and 5. The incoherent scattering crosssections of Pr and Fe are small compared to that of hydrogen.

Examples of the QENS spectra obtained with the time-of-flight and backscattering spectrometers are shown in Fig. 4. The low-temperature data showing no quasielastic signal are used as the resolution functions. As shown in Fig. 1, the tetrahedral sites in the basal plane normal to the  $c$  axis form the arrays of isolated hexagons with a side dimension of  $\approx 1.16 \text{ \AA}$ . The distance between the centers of the hexagons equals the  $a$  lattice constant ( $\approx 8.70 \text{ \AA}$  at  $300 \text{ K}$ ). Because hopping between well-separated hexagons is unlikely, we fit the QENS data with a model scattering function describing a hopping between the six sites of an isolated hexagon. The model from Ref. 23 describing the hopping between six sites on a circle of radius  $r$  was modified to allow for the fact that: (i) all three hydrogen atoms per formula unit in the octahedral sites are immobile and (ii) even a fraction of the hydrogen atoms in the tetrahedral sites is immobile. A temperature-

dependent parameter  $p(T)$  is commonly used to denote the fraction of mobile hydrogen atoms in hydrides.<sup>13–16</sup> In addition to the hydrogen atoms in the octahedral sites, the fraction of immobile hydrogen in the tetrahedral sites,  $1-p(T)$ , contributes to the elastic line. It is suggested that in nonstoichiometric hydrides, H-H interactions may result in the formation of locally ordered atomic configurations, the destruction of which at higher temperatures leads to an increase of  $p(T)$ .<sup>13–16</sup> In stoichiometric hydrides such as  $\text{Pr}_2\text{Fe}_{17}\text{H}_5$ , some H atoms at the tetrahedral sites may be trapped, for example, by antisite defects in the host lattice. The resulting model scattering function is given by

$$S_{inc}(Q, E) = \left[ \frac{3}{5} + \frac{2}{5}(1-p(T)) + \frac{2}{5}p(T)A_0(Q) \right] \delta(E) + \frac{2}{5}p(T) \times \left[ A_1(Q) \frac{1}{\pi} \frac{\Gamma_1}{E^2 + \Gamma_1^2} + A_2(Q) \frac{1}{\pi} \frac{\Gamma_2}{E^2 + \Gamma_2^2} + A_3(Q) \frac{1}{\pi} \frac{\Gamma_3}{E^2 + \Gamma_3^2} \right], \quad (1)$$

$$A_0(Q) = \frac{1}{6} [1 + 2j_0(Qr) + 2j_0(Qr\sqrt{3}) + j_0(2Qr)], \quad (2)$$

$$A_1(Q) = \frac{1}{6} [2 + 2j_0(Qr) - 2j_0(Qr\sqrt{3}) - 2j_0(2Qr)], \quad (3)$$

$$A_2(Q) = \frac{1}{6} [2 - 2j_0(Qr) - 2j_0(Qr\sqrt{3}) + 2j_0(2Qr)], \quad (4)$$

$$A_3(Q) = \frac{1}{6} [1 - 2j_0(Qr) + 2j_0(Qr\sqrt{3}) - j_0(2Qr)], \quad (5)$$

where  $j_0$  is the spherical Bessel function of zeroth order, and the Lorentzian half widths at half maximum (HWHM) are functions of the time between jumps  $\tau$

$$\Gamma_1 = 0.5 \frac{\hbar}{\tau}, \quad (6)$$

$$\Gamma_2 = 1.5 \frac{\hbar}{\tau}, \quad (7)$$

$$\Gamma_3 = 2.0 \frac{\hbar}{\tau}. \quad (8)$$

When fitting to the data, the model scattering function Eq. (1) was convolved with the instrument resolution function. We used a fixed value of  $r=1.16 \text{ \AA}$  since, for six equidistant sites on a circle, the distance between two neighboring sites is equal to the circle radius. The fitting parameters were  $p(T)$  and  $\tau$ .

Prior to modeling with the scattering function Eqs. (1)–(8), we used a simplified scattering function

$$S_{inc}(Q, E) = A(Q) \delta(E) + [1 - A(Q)] \frac{1}{\pi} \frac{\Gamma}{E^2 + \Gamma^2} \quad (9)$$

convolved with the resolution function to fit the data. Then, the parameter  $A(Q)$  extracted from the fit that represents the

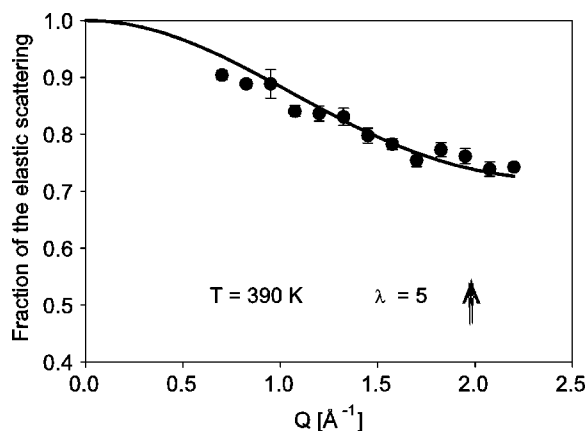


FIG. 5. The fraction of the elastic scattering obtained as  $A(Q)$  in Eq. (9) and its fitting with the expression  $A(Q) = \frac{3}{5} + \frac{2}{5}[1 - p(T)] + \frac{1}{5}p(T)\frac{1}{6}[1 + 2j_0(Qr) + 2j_0(Qr\sqrt{3}) + j_0(2Qr)]$  using a fixed  $r$  of  $1.16 \text{ \AA}$ .

$Q$  dependence of the fraction of the elastic scattering was fitted with the term in the first brackets in Eq. (1). A fixed value of  $r = 1.16 \text{ \AA}$  was used, while  $p(T)$  was the fitting parameter. The result of this fit for the 390 K data collected using a wavelength of  $5 \text{ \AA}$ , which enables a wider  $Q$  range compared to the rest of the data, is shown in Fig. 5. The reasonable agreement is suggestive of the appropriateness of the six-site jump model for describing the observed dynamics. The points at the lowest  $Q$  values exhibit the strongest deviation from the model, likely because of multiple scattering effects, which predominantly affect data at low  $Q$ .<sup>23,24</sup>

Figures 6 and 7 demonstrate the parameters obtained using the rigorous model described by Eqs. (1)–(8). The temperature dependence of the mobile fraction of hydrogen atoms in the tetrahedral sites is presented in Fig. 6. As expected,  $p(T)$  increases with temperature. The absolute values of  $p(T)$  exceed those observed at similar temperatures for nonstoichiometric hydrides such as  $\text{TaV}_2\text{H}_{0.6}$ ,  $\text{TaV}_2\text{H}_{1.1}$ ,<sup>13</sup>  $\text{ZrMo}_2\text{H}_{0.3}$ ,  $\text{ZrMo}_2\text{H}_{0.92}$ ,<sup>15</sup> and  $\text{HfMo}_2\text{H}_{0.26}$ .<sup>16</sup> We attempted to fit  $p(T)$  with the expression<sup>25</sup>

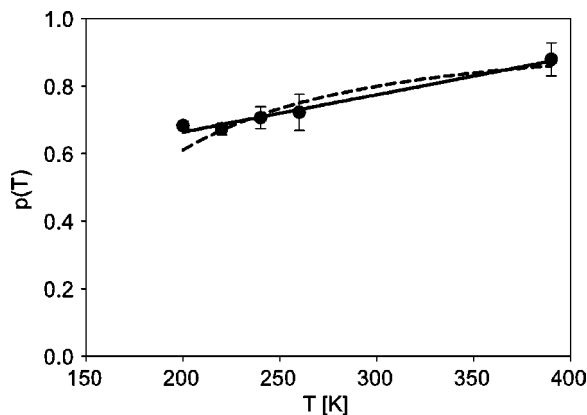


FIG. 6. The temperature dependence of  $p(T)$  (the mobile fraction of hydrogen atoms in the tetrahedral sites) fit with Eq. (10) (dashed line) and with a linear temperature function (solid line).

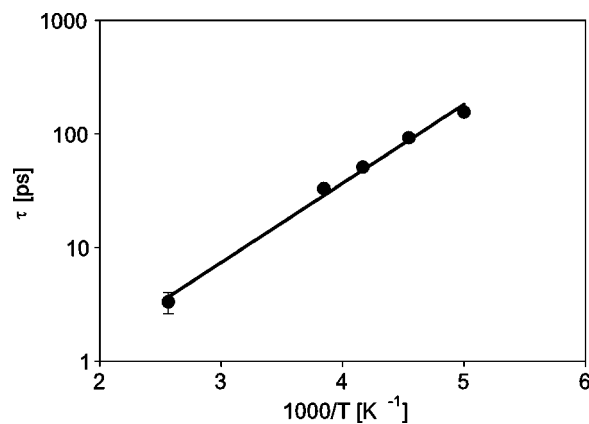


FIG. 7. The temperature dependence of the residence time between jumps fit with an Arrhenius law.

$$p(T) = \frac{g_1 \exp(-\Delta E/k_B T)}{1 + g_1 \exp(-\Delta E/k_B T)}, \quad (10)$$

where  $\Delta E$  is the energy difference between static and mobile H states, and  $g_1$  is the relative degeneracy factor. These attempts were unsuccessful until we excluded the  $T = 200 \text{ K}$  temperature point. Then we were able to obtain a fit as shown in Fig. 6 by the dashed line with the fit parameters  $\Delta E = 48.2 \text{ meV}$  and  $g_1 = 25.7$ . However, a better fit for all measured temperature points could be obtained using a linear temperature dependence of  $p(T)$ . A linear dependence of  $p(T)$  was observed in the aforementioned nonstoichiometric hydrides,<sup>13–16</sup> and was ascribed to a spread in local H configurations, which is associated with a nearly uniform distribution of  $\Delta E$  at low  $\Delta E$ . Yet, for a stoichiometric hydride such as  $\text{Pr}_2\text{Fe}_{17}\text{H}_5$ , a linear temperature dependence of  $p(T)$  seems more difficult to explain.

The temperature dependence of the residence time between jumps shown in Fig. 7 demonstrates an Arrhenius-type behavior,  $\tau = \tau_0 \exp(E_A/k_B T)$ , with  $\tau_0 = 0.06 \text{ ps}$  and  $E_A = 0.14 \text{ eV}$ . It has been suggested previously using Mössbauer spectroscopy<sup>7</sup> that two hydrogen atoms occupying the tetrahedral sites in  $\text{Pr}_2\text{Fe}_{17}\text{H}_5$  jump rapidly between available sites at and above  $155 \text{ K}$  on the Mössbauer timescale of  $100 \text{ ns}$ . Between  $155$  and  $85 \text{ K}$ , the hydrogen jumping ceased.<sup>7</sup> Using the activation energy of  $0.14 \text{ eV}$  and the pre-exponential factor of  $0.06 \text{ ps}$ , one finds  $\tau(85 \text{ K}) = 1.18 \times 10^4 \text{ ns}$  and  $\tau(155 \text{ K}) = 2.1 \text{ ns}$ , in agreement with the results obtained by Mössbauer spectroscopy. One can also estimate that at  $T \approx 170 \text{ K}$ , the time between jumps  $\tau = 820 \text{ ps}$ , which corresponds to the HFBS resolution of  $0.8 \mu\text{eV}$  in the fixed-window operation mode. As explained above, on cooling down, this temperature marks an onset of a more rapid growth of “elastic” intensity, when the spectrometer resolution becomes insufficient to separate the QENS signal from the truly elastic scattering.

It should be noted that hopping of hydrogen in the presence of two H atoms per hexagon needs to be correlated in order to satisfy the Switendick criterion of the minimum H-H separation.<sup>10</sup> As mentioned above, all but the opposite vertices of a hexagon with a side dimension of  $1.16 \text{ \AA}$  are



too close to accommodate a pair of hydrogen atoms separated by no less than 2.1 Å. With a strong H-H repulsive interaction, only the simultaneous jumps of two atoms in the same direction should be possible. The scattering law for such a completely correlated motion of a pair of H atoms is identical to that for a single jumping atom (as in the case of a dumbbell molecule).

#### IV. CONCLUSION

In Pr<sub>2</sub>Fe<sub>17</sub>H<sub>5</sub>, three hydrogen atoms per formula unit fully occupy the 9e distorted octahedral sites of the host metal lattice, while two hydrogen atoms per formula unit fill one third of the 18g tetrahedral sites. The hydrogen atoms in the octahedral sites are immobile on the time scale of the QENS measurements, while those in the tetrahedral sites perform jumps between such sites that constitute arrays of isolated hexagons in the basal plane. The residence time of H atoms between jumps shows an Arrhenius-type temperature dependence,  $\tau(\text{ps})=0.06 \times \exp(E_A/k_B T)$ , with an activation energy of 0.14 eV. The dynamics of hydrogen motion is thus observable down to  $T \approx 170$  K in a QENS experiment with a

0.8  $\mu\text{eV}$  resolution. The hydrogen jump dynamics is also in agreement with previous results of Mössbauer spectroscopy<sup>7</sup> on the timescale of 100 ns. While fast localized motion of H atoms within hexagons has been observed in nonstoichiometric hydrides with less than one atom per hexagon,<sup>13–16</sup> the high population of two H atoms per hexagon in Pr<sub>2</sub>Fe<sub>17</sub>H<sub>5</sub> might be expected to suppress the hydrogen hopping because of the strong repulsive interaction. To reconcile the dynamics of hydrogen observed in this work with the Switendick criterion of minimal hydrogen separation distance in metals,<sup>10</sup> one needs to assume that the jumps of the paired H atoms are correlated, that is, only the simultaneous jumps of two atoms in the same direction are possible.

#### ACKNOWLEDGMENTS

The authors are grateful to I. Peral for assistance with the measurements and to R. Cappelletti for valuable discussions. O.I. would like to thank G. J. Long and F. Grandjean for interesting discussions. Utilization of the DAVE package for the data analysis is acknowledged. This work utilized facilities supported in part by the National Science Foundation under Agreement No. DMR-0086210.

- 
- <sup>1</sup>O. Isnard, S. Miraglia, J. L. Soubeyrou, D. Fruchart, and A. Stergiou, *J. Less-Common Met.* **162**, 273 (1990).  
<sup>2</sup>O. Isnard, S. Miraglia, D. Fruchart, and J. Deportes, *J. Magn. Magn. Mater.* **103**, 157 (1992).  
<sup>3</sup>O. Isnard, S. Miraglia, J. L. Soubeyrou, D. Fruchart, and P. L'héritier, *J. Magn. Magn. Mater.* **137**, 151 (1994).  
<sup>4</sup>F. Grandjean, D. Hautot, G. J. Long, O. Isnard, S. Miraglia, and D. Fruchart, *J. Appl. Phys.* **79**, 4584 (1996).  
<sup>5</sup>O. Isnard, M. Guillot, S. Miraglia, and D. Fruchart, *J. Appl. Phys.* **79**, 4608 (1996).  
<sup>6</sup>F. Grandjean, D. Hautot, G. J. Long, O. Isnard, S. Miraglia, and D. Fruchart, *J. Appl. Phys.* **85**, 4654 (1999).  
<sup>7</sup>D. Hautot, G. J. Long, F. Grandjean, O. Isnard, and S. Miraglia, *J. Appl. Phys.* **86**, 2200 (1999).  
<sup>8</sup>O. Isnard, S. Miraglia, J. L. Soubeyrou, and D. Fruchart, *Solid State Commun.* **81**, 13 (1992).  
<sup>9</sup>O. Isnard, J. L. Soubeyrou, S. Miraglia, D. Fruchart, L. M. Garcia, and J. Bartolome, *Physica B* **180–181**, 629 (1992).  
<sup>10</sup>A. C. Switendick, *Z. Phys. Chem., Neue Folge* **117**, 89 (1979).  
<sup>11</sup>V. A. Yartys, R. V. Denys, B. C. Hauback, H. Fjellvag, I. I. Bulyk, A. B. Riabov, and Ya. M. Kalychak, *J. Alloys Compd.* **330–332**, 132 (2002).  
<sup>12</sup>P. Vajeeston, P. Ravindran, R. Vidya, A. Kjekshus, H. Fjellvag, and V. A. Yartys, *Phys. Rev. B* **67**, 014101 (2003).  
<sup>13</sup>A. V. Skripov, J. C. Cook, D. S. Sibirtsev, C. Karmonik, and R. Hempelmann, *J. Phys.: Condens. Matter* **10**, 1787 (1998).  
<sup>14</sup>A. V. Skripov, M. Pionke, O. Randl, and R. Hempelmann, *J. Phys.: Condens. Matter* **11**, 1489 (1999).  
<sup>15</sup>A. V. Skripov, J. C. Cook, C. Karmonik, and V. N. Kozhanov, *Phys. Rev. B* **60**, 7238 (1999).  
<sup>16</sup>A. V. Skripov, J. C. Cook, T. J. Udovic, and V. N. Kozhanov, *Phys. Rev. B* **62**, 14 099 (2000).  
<sup>17</sup>O. Isnard, A. Sippel, M. Loewenhaupt, and R. Bewley, *J. Phys.: Condens. Matter* **13**, 1 (2001).  
<sup>18</sup>O. Isnard, D. Hautot, G. J. Long, and F. Grandjean, *J. Appl. Phys.* **88**, 2750 (2000).  
<sup>19</sup>T. J. Udovic, D. A. Neumann, J. Leao, and C. M. Brown, *Nucl. Instrum. Methods Phys. Res. A* **517**, 189 (2004).  
<sup>20</sup>A. Meyer, R. M. Dimeo, P. M. Gehring, and D. A. Neumann, *Rev. Sci. Instrum.* **74**, 2759 (2003).  
<sup>21</sup>J. R. D. Copley and J. C. Cook, *Chem. Phys.* **292**, 477 (2003).  
<sup>22</sup>T. J. Udovic, E. Mamontov, O. Isnard, and J. J. Rush (unpublished).  
<sup>23</sup>M. Bée, *Quasielastic Neutron Scattering* (Hilger, Bristol, 1988).  
<sup>24</sup>See, for example, J. Wuttke, *Phys. Rev. E* **62**, 6531 (2000).  
<sup>25</sup>N. F. Berk, J. J. Rush, T. J. Udovic, and I. S. Anderson, *J. Less-Common Met.* **172**, 496 (1991).